Temperature dependent DC/RF performance of Si/SiGe resonant interband tunnelling diodes

N. Jin, S.-Y. Chung, R. Yu, P.R. Berger and P.E. Thompson

The temperature dependent DC/RF performance of Si-based resonant interband tunnelling diodes (RITDs) grown by low temperature molecular beam epitaxy was studied. Both DC and RF performance were measured at various temperatures from 20 to 150°C. At 20°C, the RITD exhibits a peak current density (J_p) of 22 kA/cm^2 with peak-to-valley current ratio (PVCR) of 2.0. The maximum resistive cutoff frequency (f_{r0}) of 2.4 GHz was obtained by biasing the diode at 320 mV. Increasing temperature slightly degrades the PVCR and f_{r0}. At 150°C, the PVCR and f_{r0} reduced to 1.8 and 1.9 GHz, respectively. The observed weak temperature dependence of the DC/RF performance and the GHz operating frequency make Si/SiGe RITDs a good candidate for high power microwave applications.

Introduction: Since Si-based resonant interband tunnelling diodes (RITDs) grown by low temperature molecular beam epitaxy (LT-MBE) were first built by Rommel *et al.* [1], numerous studies have been carried out to improve their DC performance (see [2] and references therein). With the recent demonstration of Si-based RITDs with very high peak current density of 151 kA/cm^2 [2] for high speed and high power microwave applications, it is of great interest to characterise its RF performance and study its temperature dependency, especially the RF performance at higher temperature. In this Letter, we report on the first study of temperature dependent RF performance of Si-based tunnel diodes.

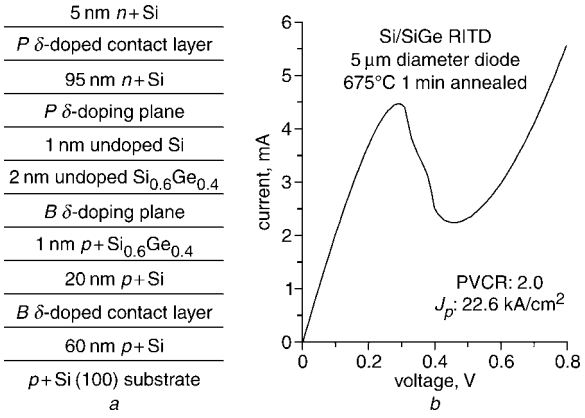

Fig. 1 *Schematic of RITD structure used in this study, and DC I-V characteristic measured at 20°C*

a Schematic of RITD structure
b DC I-V characteristic

Experiment: Fig. 1*a* shows the schematic of the RITD structure used in this study. The diode has an active layer composed of P δ-doping layer/1 nm i-Si/2 nm i-$Si_{0.6}Ge_{0.4}$/B δ-doping layer/1 nm p+-$Si_{0.6}Ge_{0.4}$. An additional P δ-doping layer was grown 5 nm below the surface of the top contact and an additional B δ-doping layer was grown 20 nm below the active region to reduce each contact resistance. The nominal doping level for both n^+ and p^+ layers is 5×10^{19} cm^{-3}, while both the B and P δ-doping sheet concentrations were maintained at 1×10^{14} cm^{-2}. The structure was grown by LT-MBE using elemental Si and Ge in electron-beam sources on 75 mm B-doped ($\rho = 0.015 - 0.04\ \Omega \cdot$ cm) Si (100) wafers. Prior to device fabrication, the as-grown wafer was rapid thermal annealed (RTA) using a forming gas ambient (N_2/H_2) at 675°C for 1 min. The diode was fabricated using standard contact photolithography. The diode mesa (5 μm diameter) was defined by etching through the *pn* junction in a $HF/HNO_3/H_2O$ solution using Ti/Au as the self-aligned etching mask. A photo-sensitive polyimide layer was then lithographically defined to open contact windows to the anode and cathode. After curing the polyimide in an N_2 ambient, the 1-port coplanar contact pads were defined by Ti/Au lift-off process.

Results: The I-V characteristics were measured at DC using an Agilent 4156C parameter analyser. As shown in Fig. 1*b*, a PVCR of 2.0 with J_p of 22.6 kA/cm^2 was obtained at 20°C. The small plateau from 310 to 400 mV is the evidence of oscillations induced when the diode was biased in that range during measurements. The RF performance was characterised using an Agilent 8510C network analyser. The 50 Ω coplanar microwave probes were calibrated by the short-open-load-through (SOLT) method before measurements. The S_{11} data of both the diodes and on-wafer open-pad test structure were measured from 100 MHz to 10 GHz in 0.1 GHz steps. The bias voltage was swept from 0 mV to 0.7 V in 10 to 50 mV steps. The small signal amplitude delivered to the diodes was estimated to be 10 mV peak-to-peak. The solid lines of Fig. 2 show the measured impedances against frequency at 250 mV (pre-peak region), 320 mV (NDR region), 420 mV (NDR region) and 700 mV (post-valley region). When the diode was biased at 320 and 420 mV, the impedances exhibit negative real parts below the f_{r0} of 2.40 and 1.68 GHz, respectively. Note, oscillations were observed at low frequency (<600 MHz) with a 320 mV biasing voltage. When the diode was biased between 330 and 390 mV, oscillations extend to the high frequency region, and no meaningful impedance curve can be obtained. The inset of Fig. 2*a* shows the f_{r0} against bias voltage. Biasing the RITD at 320 mV leads to the maximum f_{r0} of 2.40 GHz, which is higher than previously reported f_{r0} of Si-based tunnel diodes [3, 4].

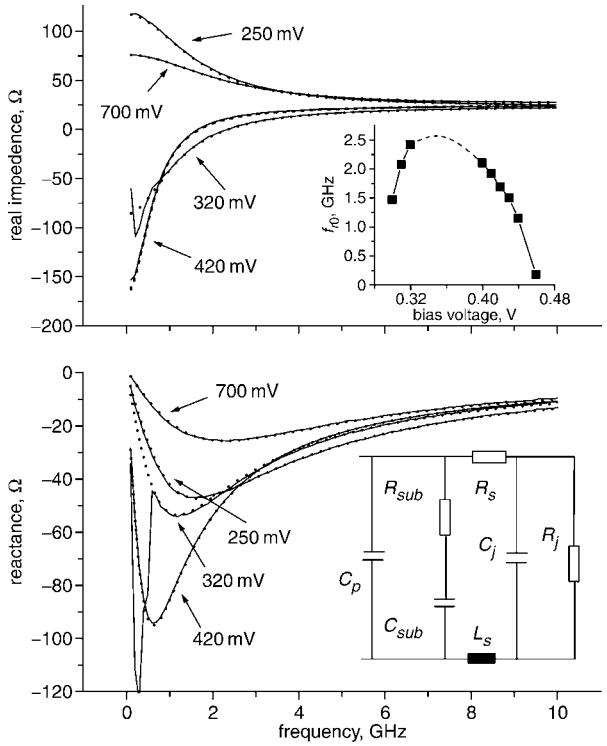

Fig. 2 *Comparison of measured impedance (solid lines) and modelled impedance (short dot lines) at four representative bias voltages*

Real components plotted in upper Figure, imaginary components plotted in lower Figure. The four bias voltages plotted are 250 mV (pre-peak region), 320 mV, 420 mV (NDR region) and 700 mV (post-valley region)
Insets: Insets in upper and lower Figures show f_{r0} against bias voltage and equivalent circuit model of studied RITD, respectively

An equivalent circuit model of the Si/SiGe RITD shown in the inset of Fig. 2*b* was used to fit the measured S_{11}. C_p represents the fringing capacitance of the probe pad. R_{sub} and C_{sub} model the loss due to the conducting Si substrate. The diode is represented by a simple circuit which consists of a series resistance (R_s), series inductance (L_s), junction capacitance (C_j), and junction resistance (R_j). Advanced Design System (ADS) software was used to fit the measured S_{11} to the simple circuit model. The fitted results at the four representative bias points are plotted in Fig. 2 as short dot lines, which are in excellent agreement with the measured values.

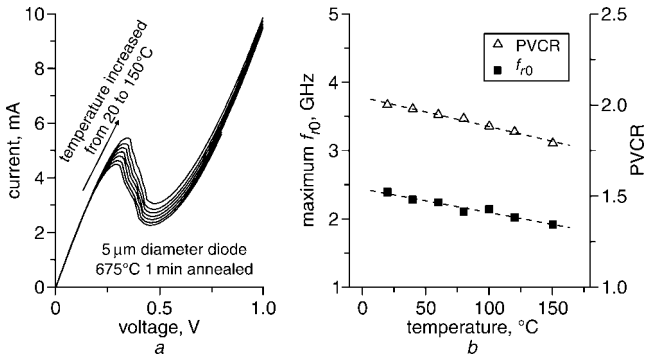

Fig. 3 *DC I-V characteristic measured at various temperatures, and PVCR and f_{r0} against temperature*

a DC I-V characteristic
b PVCR and f_{r0} against temperature

The temperature dependent DC and RF performances were measured at various temperatures (20, 40, 60, 80, 100, 120, 150°C). The I-V characteristics of a 5 μm diameter RITD are plotted in Fig. 3*a*. A set of I-V characteristics showing weak temperature dependence was observed, which indicates that tunnelling current (both desired band-to-band tunnelling current and defect-related excess current) dominates over thermal diffusion current even at a 1 V bias voltage because of the thin tunnelling barrier. Both peak current and valley current increase as a result of the narrowed bandgap as the temperature increases. The PVCR slightly decreases with increased temperature as shown in Fig. 3*b*. At 150°C, the PVCR dropped to 1.8, which is of 10.0% degradation from its room temperature PVCR. The weak temperature dependent DC performance was also reported on an Si Esaki diode with a J_p of 47 kA/cm^2 [5]. However, a large temperature dependence on the I-V characteristics was observed for the Si Esaki diode with a J_p of 112 A/cm^2 formed by spin-on dopants [6], because the thermal diffusion current component is comparable to the tunnelling current component. A weak temperature dependence on the RF performance was observed in this study and is shown in Fig. 3*b*. The maximum f_{r0} at 150°C dropped to 1.9 GHz, which corresponds to a 19.6% degradation of its room temperature value. It was observed that both the PVCR and f_{r0} are linearly dependent on temperature within the measured temperature range. Assuming the linear dependence still holds at higher temperatures, the temperature at which f_{r0} drops to 1 GHz can be projected to be 410°C.

Conclusion: We studied the temperature dependent DC/RF performance of Si-based RITDs grown by LT-MBE. At 20°C, the device shows a PVCR of 2.0 and maximum f_{r0} of 2.4 GHz; at 150°C, PVCR and maximum f_{r0} drop to 1.8 and 1.9 GHz, respectively. The weak temperature dependent DC/RF performance of Si/SiGe RITDs and its GHz operating frequency make this device attractive for high power microwave applications.

Acknowledgments: The authors thank D. Liu and W. Lu for their assistance in RF measurements. Ohio State University was supported by the National Science Foundation (OMR-0103248 and ECS-0323657). The work at NRL was supported by the Office of Naval Research.

3 January 2005
Electronics Letters online no: 20050020
doi: 10.1049/el:20050020

N. Jin, S.-Y. Chung and P.R. Berger (*Department of Electrical and Computer Engineering, The Ohio State University, Columbus, OH 43210-1272, USA*)

E-mail: pberger@ieee.org

R. Yu (*Department of Physics, The Ohio State University, Columbus, OH 43210-1106, USA*)

P.E. Thompson (*Naval Research Laboratory, Code 6812, Washington, DC 20375-5347, USA*)

P.R. Berger: Also with Department of Physics, The Ohio State University, Columbus, OH 43210-1106, USA

References

1 Rommel, S.L., *et al.*: 'Room temperature operation of epitaxially grown $Si/Si_{0.5}Ge_{0.5}/Si$ resonant interband tunneling diodes', *Appl. Phys. Lett.*, 1998, **73**, pp. 2191–2193
2 Jin, N., *et al.*: '151 kA/cm^2 peak current densities in Si/SiGe resonant interband tunneling diodes for high power mixed-signal applications', *Appl. Phy. Lett.*, 2003, **83**, pp. 3308–3310
3 Auer, U., *et al.*: 'Low-voltage MOBILE logic module based on Si/SiGe interband tunneling diodes', *IEEE Electron Device Lett.*, 2001, **22**, pp. 215–217
4 Dashiell, M.W., *et al.*: 'Low-voltage MOBILE logic module based on Si/SiGe interband tunneling diodes', *IEEE Electron Device Lett.*, 2002, **23**, pp. 357–359
5 Dashiell, M.W., *et al.*: 'Current-voltage characteristics of high current density silicon Esaki diodes grown by molecular beam epitaxy and the influence of thermal annealing', *IEEE Trans. Electron Devices*, 2000, **47**, pp. 1707–1714
6 Wang, J., *et al.*: 'Silicon tunnel diodes formed by proximity rapid thermal diffusion'. Proc. of IEEE Lester Eastman Conference on High Performance Devices, 2002, pp. 393–401